Experimental Monte Carlo Quantum Process Certification

L. Steffen, M. P. da Silva, A. Fedorov, M. Baur, and A. Wallraff

Phys. Rev. Lett. **108**, 260506 — Published 28 June 2012

DOI: 10.1103/PhysRevLett.108.260506

Experimental Monte Carlo Quantum Process Certification

L. Steffen,[1] M. P. da Silva,[2] A. Fedorov,[1] M. Baur,[1] and A. Wallraff[1]
[1] *Department of Physics, ETH Zurich, CH-8093 Zurich, Switzerland*
[2] *Disruptive Information Processing Technologies Group, Raytheon BBN Technologies, 10 Moulton Street, Cambridge, MA 02138 USA*
(Dated: May 21, 2012)

Experimental implementations of quantum information processing have now reached a level of sophistication where quantum process tomography is impractical. The number of experimental settings as well as the computational cost of the data post-processing now translates to days of effort to characterize even experiments with as few as 8 qubits. Recently a more practical approach to determine the fidelity of an experimental quantum process has been proposed, where the experimental data is compared directly to an ideal process using Monte Carlo sampling. Here we present an experimental implementation of this scheme in a circuit quantum electrodynamics setup to determine the fidelity of two qubit gates, such as the CPHASE and the CNOT gate, and three qubit gates, such as the Toffoli gate and two sequential CPHASE gates.

Introduction — Quantum process tomography [1] is a widely used method to obtain a complete description of experimental implementations of gates or algorithms. With the ongoing experimental progress and growth in system size, quantum process tomography is already impractical and will soon become infeasible in state-of-the-art experiments, since the number of experimental settings as well as the computational cost of the post-processing increases exponentially with the number of qubits. Even the most recent tomography algorithms would need days of data post-processing in order to yield a process tomography estimate for as few as 8 qubits [2].

Thanks to the linearity of quantum mechanics, a quantum process can be described by a matrix, and the purpose of quantum process tomography is to estimate this matrix. Experimentally, the determination of the process matrix for an n-qubit process involves the preparation of the qubits in 4^n linearly independent product states and the measurement of 4^n linearly independent observables, resulting in 4^{2n} expectation values which are related to the process matrix by a linear transformation. There are two major drawbacks to this approach: 1) statistical fluctuations in the measured expectation values must be dealt with in order for the estimated process matrix to be physical, 2) the resulting exponential amount of data is often reduced to a single number, the average fidelity, which quantifies the similarity between the experimental process and some ideal physical process, and thus the exponential amount of data collected is extremely redundant. The most appropriate method to produce a physical estimate from a perturbed data-set is still under active debate [3], and Monte Carlo process certification [4, 5] has been proposed as an efficient method to estimate the average fidelity of an experiment to a large class of ideal processes while completely sidestepping the exponential overhead associated with the reconstruction of process matrices.

Here we present the implementation of Monte Carlo process certification on two- and three-qubit gates in a circuit QED system [6–8] with three transmon qubits [9] coupled to a superconducting waveguide resonator. We give a detailed description of the protocol implemented with our setup and analyze the errors of the protocol. The obtained fidelities are then compared to fidelities obtained by quantum process tomography.

Background — Monte Carlo process certification [4, 5] relies on the fact that an n-qubit process $\mathcal{E}$ can be described by a $2n$-qubit density matrix $\hat{\rho}_{\mathcal{E}}$, known as the Choi matrix [10, 11]. In the case where we want to compare an experimentally realized process $\mathcal{E}_{\mathrm{exp}}$ to an ideal unitary process $\mathcal{E}_{\mathrm{ideal}}$, the fidelity expression for the two Choi matrices [12] simplifies to

$$F(\hat{\rho}_{\mathcal{E}_{\mathrm{ideal}}}, \hat{\rho}_{\mathcal{E}_{\mathrm{exp}}}) = \mathrm{tr}\left[\hat{\rho}_{\mathcal{E}_{\mathrm{ideal}}}\hat{\rho}_{\mathcal{E}_{\mathrm{exp}}}\right], \tag{1}$$

which in turn is related to the unitarily invariant average fidelity by $\overline{F} = (dF + 1)/(d + 1)$ where d is the dimension of the Hilbert space used to describe the states of the system [13]. The fidelity expression can be re-written as

$$F(\hat{\rho}_{\mathcal{E}_{\mathrm{ideal}}}, \hat{\rho}_{\mathcal{E}_{\mathrm{exp}}}) = \sum_i \Pr(i)\frac{\sigma_i}{\rho_i}, \tag{2}$$

where $\rho_i = \mathrm{tr}\left[\hat{\rho}_{\mathcal{E}_{\mathrm{ideal}}}\hat{P}_i\right]$ and $\sigma_i = \mathrm{tr}\left[\hat{\rho}_{\mathcal{E}_{\mathrm{exp}}}\hat{P}_i\right]$. Here, $\hat{P}_i$ is an orthonormal Hermitian operator basis chosen as the 4^n tensor products of the Pauli matrices and the identity and the sum (2) is taken over only the i with $\rho_i \neq 0$. The distribution $\Pr(i) = \frac{\rho_i^2}{d}$ reflects the relevance of the observation of $\hat{P}_i$ for the fidelity calculation — in particular, *observables with zero expectation value in the hypothetical ideal case do not contribute to the fidelity and need not be measured in actual experiments.* One can then estimate the fidelity by randomly sampling which observables to measure according to the relevance distribution $\Pr(i)$, and the number of observables required for an estimate with error ϵ is independent of n [4, 5], unlike tomography which would require 4^{2n} different experiments. The scaling of the precision with which each observable must be measured depends on the process in question, but for Clifford group [14, 15] operations such as CNOT and CPHASE, this scaling is independent of the number of qubits.

Experimental setup — The straightforward implementation of Monte Carlo process certification as described above is rather impractical, since the preparation of the state $\hat{\rho}_{\mathcal{E}}$, representing the Choi matrix of the process $\mathcal{E}$, would require preparing the maximally entangled state $|\phi\rangle = \frac{1}{\sqrt{d}}\sum_{i=1}^{d}|i\rangle\otimes|i\rangle$, where $d=2^n$ the dimension of the state Hilbert space, to obtain $\hat{\rho}_{\mathcal{E}} = (\mathbb{1}\otimes\mathcal{E})(|\phi\rangle\langle\phi|)$. This requires $2n$ qubits for an n-qubit gate, as well as perfect storage of the n ancillary qubits.

A more experimentally relevant approach is to prepare and measure only the n-qubit states on which $\mathcal{E}$ acts [4, 5]. The key idea is that the effect of the measurement of the first half of the state $|\phi\rangle$, on which no gate is applied, corresponds to a projection of the second half of the state $|\phi\rangle$ onto complex conjugates (in the computational basis) of eigenstates of the first half of the measurement operator. The measurement of $\hat{\rho}_{\mathcal{E}}$ with randomly chosen operators $\hat{A}\otimes\hat{B}$, where $\hat{A},\hat{B}$ are tensor products of n Pauli matrices or identities, can be expressed as

$$\begin{aligned}\mathrm{tr}\left[(\hat{A}\otimes\hat{B})\hat{\rho}_{\mathcal{E}}\right] &= \mathrm{tr}\left[(\hat{A}\otimes\hat{B})(\mathbb{1}\otimes\mathcal{E})(|\phi\rangle\langle\phi|)\right]\\ &= \frac{1}{d}\sum_{i=1}^{d} a_i \mathrm{tr}\left[\hat{B}\ \mathcal{E}(|a_i\rangle\langle a_i|)\right]. \qquad (3)\end{aligned}$$

Here $|a_i\rangle$ is the complex conjugate of the i^{th} eigenstate of the operator $\hat{A}$ with eigenvalue a_i. This final expression corresponds to the action of the process $\mathcal{E}$ on the state $|a_i\rangle$ followed by a measurement of the observable $\hat{B}$. The results for different input eigenstates are then summed up to obtain an estimate of $\mathrm{tr}\left[(\hat{A}\otimes\hat{B})\hat{\rho}_{\mathcal{E}}\right]$.

Our system — The implementation of the Monte Carlo process certification protocol was performed in a superconducting quantum processor consisting of three transmon qubits coupled to a coplanar waveguide resonator. The sample used is the same as the one in Refs. [16, 17].

Our 3-qubit system is small enough such that we can measure all relevant operators and do not need to resort to random sampling. This still allows for a significant saving in the number of measurements because many of the measurements required to perform process tomography are irrelevant for the fidelity estimate. In other words, we measure all operators which have a non-zero expectation value for the ideal gate, and calculate the accordingly weighted average to compute the gate fidelity.

The protocol requires the preparation of qubits in eigenstates of Pauli operators $\hat{A}$ and the measurement of Pauli operators $\hat{B}$. The preparation of the qubit input states is straightforward by using amplitude and phase controlled coherent microwave pulses applied to the individual charge control lines. In our setup, the implementation of the measurement using joint dispersive readout [18] of all qubits is a more complex procedure. The measurement operator is

$$\hat{M} = \sum_{i_1,\ldots,i_n\in\{0,1\}} \alpha_{i_1,\ldots,i_n}|i_1\rangle\langle i_1|\otimes|i_2\rangle\langle i_2|\otimes\cdots\otimes|i_n\rangle\langle i_n|, \qquad (4)$$

where $|0\rangle,|1\rangle$ are the computational basis states. The coefficients $\alpha_{i_1,\ldots,i_n}$ are obtained from measurements of the resonator transmission amplitude for each computational basis state [18–20]. $\hat{M}$ expressed in terms of individual qubit identity and $\hat{\sigma}_z$ Pauli operators is

$$\hat{M} = \sum_{\hat{j}_1,\ldots,\hat{j}_n\in\{\mathbb{1},\hat{\sigma}_z\}} \beta_{j_1,\ldots,j_n}\hat{j}_1\otimes\hat{j}_2\otimes\cdots\otimes\hat{j}_n, \qquad (5)$$

with coefficients $\beta_{j_1,\ldots,j_n}$ calculated as combinations of the $\alpha_{i_1,\ldots,i_n}$. By averaging many measurement outcomes of the same operator, we are able to perform a measurement of the expectation value of the operator in question.

In general the measurement operator has 2^n different elements. However, in Monte Carlo process certification for each input state the expectation value of only one specific element is needed. This element can be obtained by adding measurement outcomes with different signs of $\hat{\sigma}_z$ operators of different qubits, realized by π pulses applied to the corresponding qubits just before the measurement. Since the first element $\mathbb{1}\otimes\cdots\otimes\mathbb{1}$ has always an expectation value of one, one needs to measure 2^{n-1} different expectation values to extract a single operator $\hat{B}$. We emphasize that this particular property and the overhead associated with it relate to our joint readout, and are not a consequence of the Monte Carlo certification method.

As an example, the joint readout procedure of the operator $\hat{\sigma}_y\otimes\hat{\sigma}_x$ for two qubits is presented in the following. The joint readout operator is $\hat{M} = \alpha_{00}|0\rangle\langle 0|\otimes|0\rangle\langle 0| + \alpha_{01}|0\rangle\langle 0|\otimes|1\rangle\langle 1| + \alpha_{10}|1\rangle\langle 1|\otimes|0\rangle\langle 0| + \alpha_{11}|1\rangle\langle 1|\otimes|1\rangle\langle 1|$, which is equivalent to $\hat{M} = \beta_{00}\mathbb{1}\otimes\mathbb{1} + \beta_{01}\mathbb{1}\otimes\hat{\sigma}_z + \beta_{10}\hat{\sigma}_z\otimes\mathbb{1} + \beta_{11}\hat{\sigma}_z\otimes\hat{\sigma}_z$. The prefactors β_{ij} are determined from measurements of the α_{ij} as described above. To measure the given combination of Pauli operators, we rotate accordingly the measurement basis of the individual qubits. For the example above, we apply a $-\pi/2$ rotation around the x-axis to the first qubit and a $\pi/2$ rotation around the y-axis to the second qubit. The resulting measurement operator is $M = \beta_{00}\mathbb{1}\otimes\mathbb{1} + \beta_{01}\mathbb{1}\otimes\hat{\sigma}_x + \beta_{10}\hat{\sigma}_y\otimes\mathbb{1} + \beta_{11}\hat{\sigma}_y\otimes\hat{\sigma}_x$. To extract only the last term in the measurement operator, a second measurement with an additional π pulse on both qubits is performed. This results in a measurement operator with two minus signs: $M = \beta_{00}\mathbb{1}\otimes\mathbb{1} - \beta_{01}\mathbb{1}\otimes\hat{\sigma}_x - \beta_{10}\hat{\sigma}_y\otimes\mathbb{1} + \beta_{11}\hat{\sigma}_y\otimes\hat{\sigma}_x$. Adding the measurement outcomes of the two experiments (for the same input state) gives the expectation value for the operator $2\left(\beta_{00}\mathbb{1}\otimes\mathbb{1} + \beta_{11}\hat{\sigma}_y\otimes\hat{\sigma}_x\right)$. Since the expectation value for $\mathbb{1}\otimes\mathbb{1}$ is always equal to 1 and β_{00} and

β_{11} are known, the expectation value of $\hat{\sigma}_y \otimes \hat{\sigma}_x$ can be extracted in this way.

Hence, it is possible in our experiments to extract any expectation value of two-qubit Pauli operators from two measurements or three-qubit Pauli operators from four measurements, using the corresponding single qubit rotations. Having found the expectation values $\sigma_i = \mathrm{tr}\left[\hat{\rho}_{\mathcal{E}_{\mathrm{exp}}} \hat{P}_i\right]$, the fidelity can be directly calculated according to Eq. (2).

According to Eq. (3), a measurement of one of the expectation values σ_i consists of averaging measurement outcomes over different input states. To achieve this, one can also perform a Monte Carlo sampling of which eigenvectors to prepare as input states. The weighting factor for the sampling is given by the absolute value of the eigenvalue. Since the system size is small in our experiments but a high accuracy is desired, we measured all eigenstates.

Results — The protocol has been tested on a 2-qubit CNOT and CPHASE gate [21, 22], on a 3-qubit Toffoli gate [17, 23], and on the sequential application of two CPHASE gates on three qubits. The CNOT and the CPHASE gates are particularly interesting for Monte Carlo process certification, since they map elements of the Pauli group to other elements of the Pauli group. Such gates are Clifford operations and their Choi matrices are stabilizer states [14, 15] for which the number of relevant Pauli operators is minimal with uniform relevance distribution. For any stabilizer state $\hat{\rho}_{\mathcal{E}}$ there is a subgroup S of the Pauli group with elements $\hat{S}_i$ such that the pure state corresponding to $\hat{\rho}_{\mathcal{E}_{\mathrm{ideal}}}$ is an eigenvector of all $\hat{S}_i$ with eigenvalue $+1$. The expectation value of each operator in this stabilizer group is $+1$. Therefore, the relevance distribution $\Pr(i) = 1/4^n$ is uniform for all $i \in \{1, \ldots, 4^n\}$. All other operators of the Pauli group have expectation value zero, and therefore have no impact on the estimation of the fidelity of a gate.

All experimentally realized gates have been characterized by calculation of their fidelity using Monte Carlo process certification (F_{MC}), unconstrained tomography data (F_{tom}), and tomography data constrained by maximum-likelihood estimation (F_{ML}).

The CNOT gate, which changes the state of a target qubit if the control qubit is in the state $|1\rangle$, is described by a Choi matrix whose stabilizer group is generated by

$$\begin{array}{rcllll} M_1 &=& \hat{\sigma}_x & \mathbb{1} & \hat{\sigma}_x & \hat{\sigma}_x, \\ M_2 &=& \hat{\sigma}_z & \mathbb{1} & \hat{\sigma}_z & \mathbb{1}, \\ M_3 &=& \mathbb{1} & \hat{\sigma}_x & \mathbb{1} & \hat{\sigma}_x, \\ M_4 &=& \mathbb{1} & \hat{\sigma}_z & \hat{\sigma}_z & \hat{\sigma}_z. \end{array} \quad (6)$$

This indicates that, e.g. eigenstates of the $\hat{\sigma}_x \otimes \mathbb{1}$ operator are mapped to eigenstates of the $\hat{\sigma}_x \otimes \hat{\sigma}_x$ operator by the CNOT operation. A visualization of the expectation value of the 16 Pauli operators with non-vanishing relevance distribution is shown in Fig. 1(a). For the present gate, the total number of different measurement settings is 120, since for each of the 15 non-unity Pauli operators we prepare 4 different input states and measure 2 different operators (required only by the joint readout). In contrast, the total number of different measurement settings for process tomography is $4^{(2\times2)} = 256$.

The CPHASE gate, which changes the phase of the $|1\rangle$ state of the target qubit by π if the control qubit is in the state $|1\rangle$, has been characterized in a way similar to the CNOT gate as these gates are locally equivalent.

A sequence of 2 CPHASE gates first acting on qubits 1 and 2, and then on qubits 2 and 3 was characterized as an example of a 3-qubit gate with a stabilizer state Choi matrix. This Choi matrix has $4^3 = 64$ Pauli operators with non-vanishing expectation value. For each of these operators we sample over 8 different eigenvectors by measuring 4 different operator combinations (again, required only by the joint readout), in total 2016 different measurement settings, again without making use of random sampling. In contrast, process tomography for any three-qubit gate requires $4^{2\times3} = 4096$ different measurement settings.

Our implementation of the Toffoli gate [17] was also characterized by Monte Carlo process certification and process tomography. The Choi matrix of the Toffoli gate is not a stabilizer state. Therefore, the list of relevant Pauli operators has no group structure and the relevance distribution $\Pr(i)$ is not uniform. We find that there are 232 Pauli operators with non-zero expectation value of 1 or ± 0.5 out of 4096 possible ones. The total number of different relevant experimental settings is $231 \times 8 \times 4 = 7392$.

Even without random sampling, the total number of measurements (including repeated measurements used for averaging) to achieve a smaller error is less for Monte Carlo process certification than for process tomography. For the Monte Carlo process estimation, we averaged each measurement setting $\sim 330\,000$ times, resulting in a total number of $\sim 2.4 \times 10^9$ measurements and an error of the fidelity of 0.5%, whereas for the process tomography we averaged each measurement setting for $\sim 790\,000$ times, resulting in a total number of $\sim 3.2 \times 10^9$ measurements and an error of the fidelity of 3%. The measurement outcomes for the different operators are shown in Fig. 1(b).

All resulting fidelities are summarized in Table I. Errors are stated as 90% confidence intervals. For Monte Carlo process estimation the error was calculated by Gaussian error propagation of the errors of the single measurements. For the error of the process tomography, the confidence interval of the distribution of fidelities was calculated based on a resampling of the measurement outcomes according to the inferred error statistics of the experiments. All the fidelities found with Monte Carlo process certification have tighter error bars than the fidelities obtained from process tomography. This is

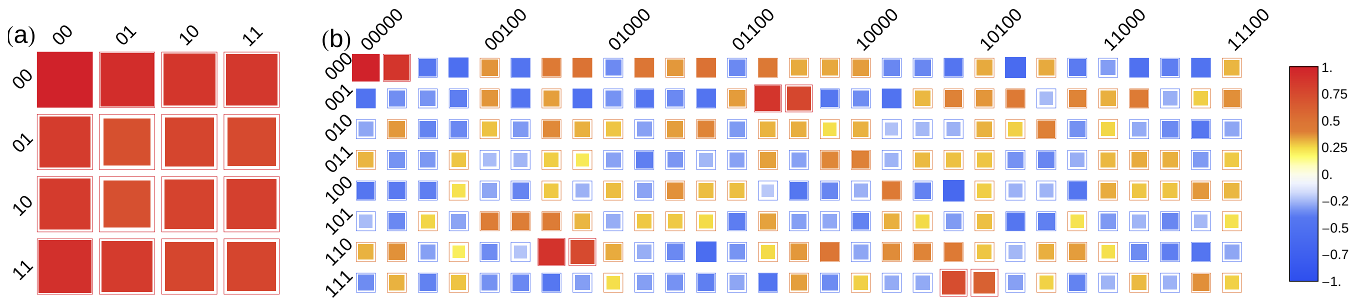

FIG. 1. Measured expectation values of all the relevant observables of the (a) CNOT gate and (b) TOFFOLI gate Choi matrices. The thin border shows the ideal expected values, the colored squares are the estimated values extracted from measurements. The $(00, 00)$ and $(000, 00000)$ entries are the expectations of the identity, so they have areas corresponding to absolute value 1 and the area of the other squares are adjusted proportionally. The column label corresponds to the most-significant digits of the binary expansion of the index of the observable, while the row label corresponds to the least significant digits (see supplementary information).

mainly due to the fact that the postprocessing for the Monte Carlo certification only consists of averaging the relevant measured values whereas full process tomography must impose collective physical constraints on the entire data set, and errors on the irrelevant observables can only add to the errors relating to the relevant observables.

As discussed before, the significant advantage of Monte Carlo process estimation is that one can estimate the fidelity of a process also without sampling over all relevant Pauli operators, on the expense of a higher uncertainty. If all relevant Pauli operators have been measured like in our experiments, the only error in the fidelity is due to the experimental uncertainty in the estimation of the different expectation values. In the case that an incomplete set of Pauli operators is sampled, there is an additional error. An asymptotic bound for this error is calculated in the supplementary material of Ref. [5], and it is shown that these bounds scale polynomially with the number of measured samples. However, the bounds are not tight and therefore too pessimistic to be used in the calculation of error bars. The error in the fidelity estimate when performing non-exhaustive sampling of the Pauli operators can be obtained by non-parametric resampling methods such as *bootstrapping* [24]. However, given that we have measured all the relevant Pauli operators for each of the gates we characterized, we can simply gather statistics

Gate	$F_{\rm MC}$	$F_{\rm tom}$	$F_{\rm ML}$
CNOT	$81.7 \pm 2.1\%$	$80 \pm 3\%$	$79 \pm 3\%$
CPHASE	$86.6 \pm 3.0\%$	$86 \pm 4\%$	$83 \pm 4\%$
2 CPHASES	$65.0 \pm 0.8\%$	$67 \pm 5\%$	$67 \pm 5\%$
Toffoli	$68.5 \pm 0.5\%$	$70 \pm 3\%$	$69 \pm 3\%$

TABLE I. Fidelities obtained by Monte Carlo process certification ($F_{\rm MC}$) compared to the values obtained with process tomography ($F_{\rm tom}$) and subsequent application of a maximum likelihood algorithm ($F_{\rm ML}$).

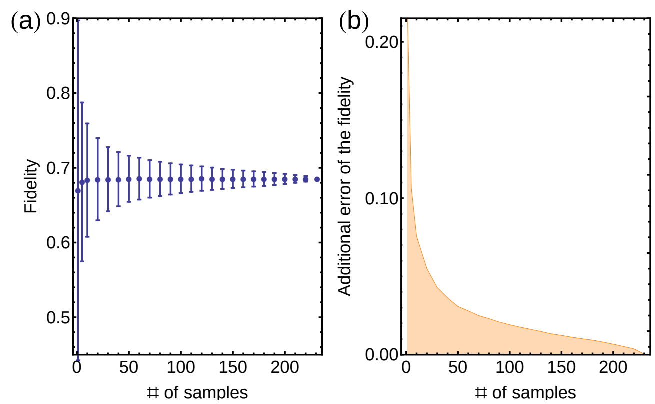

FIG. 2. (a) Mean of the estimated average output fidelity of a Toffoli gate as a function of the number of sampled observables. The error bars correspond to the 90% confidence intervals, which in turns gives an estimate of the additional error due to the non-exhaustive sampling of relevant observables. (b) The half-width of the 90% confidence intervals vs. the corresponding number of samples.

for estimates with non-exhaustive sampling. The corresponding data for the Toffoli gate is shown in Fig. 2. For our data one gets e. g. an additional error of 2% if one only samples 100 Pauli operators or an additional error of 3.2% for sampling only 50 Pauli operators. This illustrates that Monte Carlo sampling leads to significant reduction in the number of measurements required to achieve a given error bound on the fidelities.

Conclusion — We showed how Monte Carlo process certification can be implemented experimentally in a system with three qubits and joint readout. This scheme is generic and readily applicable to any qubit system. We characterized the fidelity of two 2-qubit- and two 3-qubit gates. All estimates of the gate fidelity for each of the four gates are consistent, although Monte Carlo process certification gives more accurate estimates of the fidelity using fewer measurements. This shows that Monte Carlo process certification can be used as an independent proof of the fidelity.

This work was supported by the Swiss National Science Foundation (SNF), the EU IP SOLID, and ETH Zurich.

[1] M. A. Nielsen and I. L. Chuang, *Quantum Computation and Quantum Information* (Cambridge University Press, 2000).
[2] J. A. Smolin, J. M. Gambetta, and G. Smith, Phys. Rev. Lett. **108**, 070502 (2012).
[3] R. Blume-Kohout, New Journal of Physics **12**, 043034 (2010).
[4] S. T. Flammia and Y.-K. Liu, Phys. Rev. Lett. **106**, 230501 (2011).
[5] M. P. da Silva, O. Landon-Cardinal, and D. Poulin, Phys. Rev. Lett. **107**, 210404 (2011).
[6] A. Wallraff, D. I. Schuster, A. Blais, L. Frunzio, R.-S. Huang, J. Majer, S. Kumar, S. M. Girvin, and R. J. Schoelkopf, Nature **431**, 162 (2004).
[7] A. Blais, R.-S. Huang, A. Wallraff, S. M. Girvin, and R. J. Schoelkopf, Phys. Rev. A **69**, 062320 (2004).
[8] R. J. Schoelkopf and S. M. Girvin, Nature **451**, 664 (2008).
[9] J. Koch, T. M. Yu, J. Gambetta, A. A. Houck, D. I. Schuster, J. Majer, A. Blais, M. H. Devoret, S. M. Girvin, and R. J. Schoelkopf, Phys. Rev. A **76**, 042319 (2007).
[10] A. Jamiołkowski, Rep. Math. Phys. **3**, 275 (1972).
[11] M.-D. Choi, Linear Algebra and its Applications **10**, 285 (1975).
[12] B. W. Schumacher, Phys. Rev. A **54**, 2614 (1996).
[13] M. Horodecki, P. Horodecki, and R. Horodecki, Phys. Rev. A **60**, 1888 (1999).
[14] D. Gottesman, *Stabilizer Codes and Quantum Error Correction*, Ph.D. thesis, California Institute of Technology (1997).
[15] D. Gottesman and I. L. Chuang, Nature **402**, 390 (1999).
[16] M. Baur, A. Fedorov, L. Steffen, S. Filipp, M. P. da Silva, and A. Wallraff, Phys. Rev. Lett. **108**, 040502 (2012).
[17] A. Fedorov, L. Steffen, M. Baur, M. P. da Silva, and A. Wallraff, Nature **481**, 170 (2012).
[18] S. Filipp, P. Maurer, P. J. Leek, M. Baur, R. Bianchetti, J. M. Fink, M. Göppl, L. Steffen, J. M. Gambetta, A. Blais, and A. Wallraff, Phys. Rev. Lett. **102**, 200402 (2009).
[19] R. Bianchetti, S. Filipp, M. Baur, J. M. Fink, C. Lang, L. Steffen, M. Boissonneault, A. Blais, and A. Wallraff, Phys. Rev. Lett. **105**, 223601 (2010).
[20] R. Bianchetti, S. Filipp, M. Baur, J. M. Fink, M. Göppl, P. J. Leek, L. Steffen, A. Blais, and A. Wallraff, Phys. Rev. A **80**, 043840 (2009).
[21] F. W. Strauch, P. R. Johnson, A. J. Dragt, C. J. Lobb, J. R. Anderson, and F. C. Wellstood, Phys. Rev. Lett. **91**, 167005 (2003).
[22] L. DiCarlo, J. M. Chow, J. M. Gambetta, L. S. Bishop, B. R. Johnson, D. I. Schuster, J. Majer, A. Blais, L. Frunzio, S. M. Girvin, and R. J. Schoelkopf, Nature **460**, 240 (2009).
[23] T. C. Ralph, K. J. Resch, and A. Gilchrist, Phys. Rev. A **75**, 022313 (2007).
[24] B. Efron, Biometrika **68**, 589 (1981).